Int. J. Electrochem. Sci., 17 **(2022)** Article Number: 22048, doi: 10.20964/2022.04.27

International Journal of
ELECTROCHEMICAL
SCIENCE
www.electrochemsci.org

Photoelectrochemical sensor based on nickel phthalocyanine–based metal–organic framework for sensitive detection of Curcumin

Jianwen Xiong[1,2,3*], *Wei Tan*[1,2,3],*Jinyuan Cai*[1,2,3], *Kailing Lu*[1,2,3], *Xiyu Mo*[1,2,3]

[1] Department of Food and Chemical Engineering, Liuzhou Institute of Technology, Liuzhou, Guangxi, China, 545616;
[2] Liuzhou Key Laboratory of Plant-derived Ingredients of Liuzhou river snails rice noodle, Liuzhou, Guangxi,China,545616
[3] Liuzhou Special Food Flavor and Quality Control Research Center of Engineering Technology, Liuzhou, Guangxi, China, 545616
[*]E-mail: lzsjxjw@126.com

Received: 6 December 2021 / *Accepted:* 5 February 2022 / *Published:* 4 March 2022

A novel photoelectrochemical (PEC) sensor based on a nickel phthalocyanine-based metal organic framework (NiPc–Ni MOF) was prepared and used to detect Curcumin. The photosensitive material NiPc–Ni MOF was synthesized and characterized via scanning electron microscopy, transmission electron microscopy, and X-ray diffraction. Under white light irradiation, the NiPc–Ni MOF composite modified indium tin oxide glass electrode showed a good photocurrent response to the detection of Curcumin. The experimental conditions of a light source, pH, bias voltage, modifier concentration, and coating amount were optimized. The improved PEC sensor showed a linear range of 0.0025–16 μM and a detection limit of 0.8 nM. Moreover, the PEC sensor exhibited good stability, selectivity, and reproducibility. Finally, the PEC sensor was used to detect Swisse Curcumin tablets with satisfactory results. The method presented in this study is a new strategy for detecting Curcumin.

Keywords: photoelectrochemical sensor, metal–organic frameworks, Curcumin

1. INTRODUCTION

The development of analytical disciplines has led to an increase in the number of an analytical techniques. Among them, photoelectrochemical (PEC) analysis is a novel analytical method that has been applied in drug analysis[1]. PEC sensors exhibit high sensitivity, good stability, convenient operation, and low cost[2]. PEC analytical techniques have been applied widely due to the development of several PEC activity materials, such as phthalocyanine[3-5], metal organic

frameworks[6], and porphyrin[7].

Curcumin, chemically called 1,7-bis (4-hydroxy-3-methoxyphenyl)-1,6-heptadiene-3,5-dione, is a phytochemical derived from turmeric root, is used as a food preservative, spice, and flavoring agent[8]. In recent years, Curcumin has become a focus of researches because of its anti-cancer[9], anti-inflammatory[10], and antioxidant[11] effects. To date, various methods for detecting Curcumin, such as high-performance liquid chromatography (HPLC)[12], spectroscopy[13], fluorometric measurement[14], resonance light scattering[15], and electrochemical[16-19], hvae been reported. However, the use of these methods in in-field monitoring or emergency testing is limited due to the expensive equipment, time-consuming sample preparation, and the need for trained technicians. In contrast, the use of PEC sensors have become a common analytical technique because of their simple operation, low cost, and fast analysis speed.

Metal–organic frameworks (MOFs) have attracted considerable attention. MOFs are branched coordination polymers comprised an inorganic metal and organic linker[20]. So far, MOFs bave been synthesized by various methods, such as hydrothermal, electrochemical, solvent, and microwave-assisted methods. MOFs have a advantages of large specific surface area, high porosity, and easy functionalization[21]. These advantages give MOFs a wide range of applications in adsorption[22], energy storage[23], and biosensors[24]. Carbon nanotubes and graphene are used extensively as electrode materials due to their large specific surface area and extraordinary electrical properties[25-27]. Nanocomposites of graphene and MOFs are commonly used in electrochemical sensing devices, owing to the synergistic effect caused by the highly conductive sensing component of graphene and highly surface area and adsorption capacity of MOFs[28-30]. The combination of porphyrin with a MOF can improve the photocatalysis and the electrical conductivity of the MOF[31-33]. Phthalocyanine metal (MPc) complexes are organic semiconductor molecules similar in structure to porphyrin that have been implemented widely as photosensitizers and electrocatalysts in solution[34-35]. To the best of our knowledge, there are few reports of MOFs modified using MPc and then applied to PEC sensors to detect Curcumin.

There are limited reports on PEC strategies for detecting Curcumin. In the present study, a novel material was developed and used to broaden the application in PEC sensing field. A PEC sensor based on the synthesized and characterized nickel phthalocyanine-based MOF (NiPc–Ni MOF) composite material was used to detect Curcumin. The sensor has good selectivity and stability, highlighting its development prospect in the detection of Curcumin.

2. EXPERIMENTAL SECTION

2.1. Instruments

Scanning electron microscopy (SEM, EVO18, Germany), X-ray diffraction (XRD, Bruker D8 Advance, Germany), transmission electron microscopy (TEM, FEI Tecnai F20, America), and Fourier transform infrared (FTIR) spectrometry (Perkin Elmer Co., Ltd. America) were used to characterize the NiPc–Ni MOF composite material. All PEC tests conducted on a CHI 760e electrochemical

workstation (Chenhua Instrument Co., Ltd., Shanghai, China).

2.2 Reagents

1,2-dibromo-4,5-dimethyl ether was purchased from Bidepharm (Shanghai, China). N, N-dimethylformamide (DMF), acetone, ether, and trichloromethane were obtained from Chengdu Cologne Chemical Co., Ltd. (Chengdu, China). Nickel chloride hexahydrate was acquired from Shanghai WoKai Biotechnology Co., Ltd. (Shanghai, China). Boron tribromide, dimethyl sulfoxide, and Curcumin were obtained from Shanghai Aladdin Biochemical Technology Co., Ltd. (Shanghai, China). Nickel acetate was supplied by Tianjin Guangfu Fine Chemical Research Institute (Tianjin, China). Urea was procured from Guangdong Guanghua Sci-Tech Co., Ltd. (Guangdong, China). Ammonium molybdate was acquired from Tianjin Chemical Reagent Factory No. 4 Kaida chemical plant (Tianjin, China). Phosphate buffer solutions (PBS) were carried out with a pHS-25 pH-meter (Shanghai Leici Instrument Plant, China) at room temperature.

2.3 Synthesis of 1,2-dicyano-4,5-dimethoxybenzene

1,2-dibromo-4,5-dimethoxybenzene (10.00 g) and cuprous cyanide (9.00 g) were added into 150 mL DMF. The resulting mixture was stirred at 165℃ under reflux for 5 h, and than cooled naturally. Subsequently, 300 mL of ammonia was added slowly to the brown mixture and stirred for 12 h at room temperature, followed by filtration. The filter cake was washed with a small amount of diluted ammonia (ammonia:water = 10:90), and then washed with a large amount of distilled water until it become neutral. The resulting material was removed with ether for 5 days at 55℃ after drying at 75℃ for 24 h. After extraction, the product was dried and recrystallized in methanol. Finally, the resulting material was filtered and vacuum dried at 40℃ for 12 h.

2.4 Synthesis of 2,3,9,10,16,17,23,24-octet methoxy nickel phthalocyanine ($[OMe]_8$NiPc)

1,2-dicyano-4,5-dimethoxybenzene (1.00 g), urea (320 mg), and nickel chloride hexahydrate (316 mg) were used as raw materials and ammonium molybdate (70 mg) as a catalyst, All these reagents were added into 15 mL of glycol and stirred under reflux for 4 days at 180℃ under the protection of nitrogen. The reaction product was cooled down to room temperature and then washed five times sequentially with distilled water, acetone, and chloroform. Subsequently, the product was dried in vacuum at 60℃ for 36 h to obtain a dark green solid.

2.5 Synthesis of 2,3,9,10,16,17,23,24-octa-hydroxynickel phthalocyanine ($[OH]_8$NiPc)

$(OMe)_8$NiPc (1.20 g), used as raw material, and 50 mL of methylene chloride were added into 5.7 mL of boron tribromide under the protection of nitrogen, and stirred continuously for 6 days at room temperature in the dark. After the reaction, 100 mL of distilled water was added to the mixture.

The precipitate was collected by centrifugation and washed five times with anhydrous methanol. Finally, a dark green solid was obtained by vacuum drying at 65℃ for 12 h.

2.6 Synthesis of NiPc–Ni MOF

$(OH)_8$NiPc (140 mg), used as raw material, 124.4 mg of $Ni(OAc)_2{\cdot}4H_2O$ and 2.4 mL of $NH_3{\cdot}H_2O$ were added into 24 mL of distilled water and ultrasonicated for 10 min. The resulting mixture was maintained under reflux at 85℃ for 24 h. The mixture was cooled to room temperature and washed sequentially with DMSO/$NH_3{\cdot}H_2O$ (V/V = 10:1), distilled water, and acetone. Finally, the black solid was obtained by drying at 65℃ for 24 h in the vacuum drying oven. Scheme 1 shows the final synthesis mechanism.

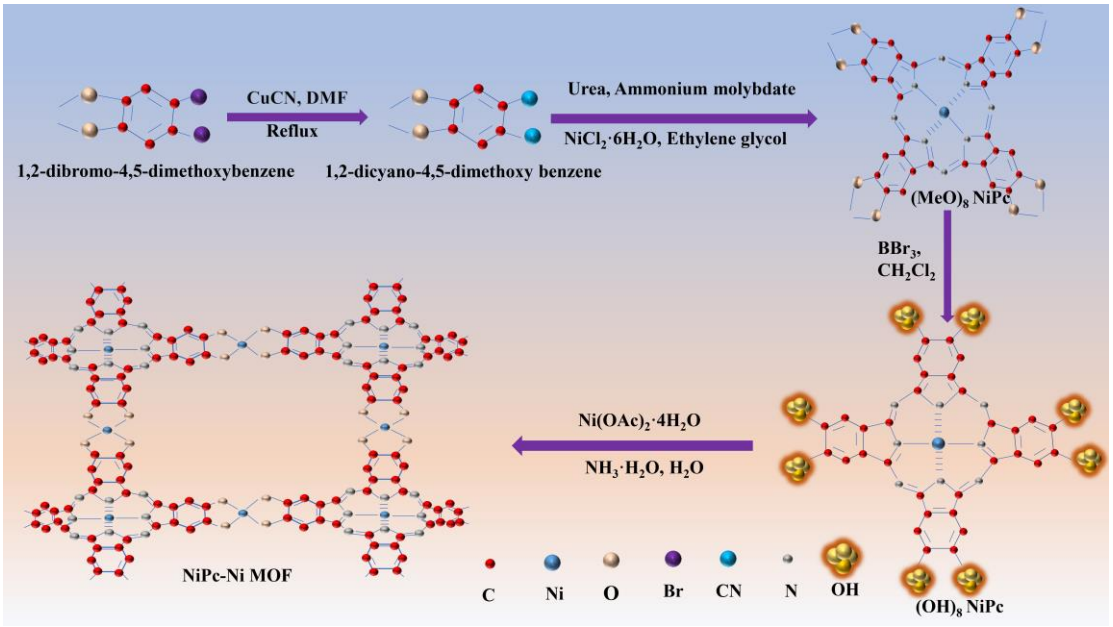

Scheme 1. The process of synthesizing NiPc–Ni MOF

2.7 Fabrication of the modifying electrode

The synthesized NiPc–Ni MOF composite material was modified on the indium tin oxide (ITO) electrode and used as the working electrode. In addition, the Pt electrode was used as an auxiliary electrode and the Ag/AgCl electrode was used as the reference electrode. Before preparing the modified electrode, the ITO electrode was cleaned ultrasonically with acetone, ethanol, and distilled water for 15 min each and then dried under an infrared lamp.1 mg of NiPc–Ni MOF material was dissolved ultrasonically in 1 mL of DMF. The resulting solution was dropped on a cleaned ITO electrode and dried at room temperature to obtain the NiPc–Ni MOF modified ITO electrode (NiPc–Ni MOF/ITO). The same method was used to prepare $(OH)_8$NiPc/ITO. All PEC experiments were performed at room temperature. As a blank comparison, DMF was dropped onto an ITO electrode to prepare bare/ITO.

2.8 Photoelectrochemical detection

NiPc-Ni MOF/ITO was used to prepare a PEC sensor to detect Curcumin. Scheme 2 presents a diagram of the possible detection mechanisms for the PEC sensor. NiPc–Ni MOF was coated on the ITO electrode, the resulting electrode absorbed light energy and produced electron-hole pairs (e^-/h^+). Electrons excited to the conduction band flowed from the ITO electrode to an external circuit, resulting in a photocurrent[36]. Subsequently, when Curcumin was added to the electrolyte, electrons migrated from the valence band (VB) to the CB. Curcumin acted as an electron acceptor in the electrolyte to inhibit e^-/h^+ recombination. Therefore, different Curcumin concentrations in the electrolyte can produce typical photocurrent responses.

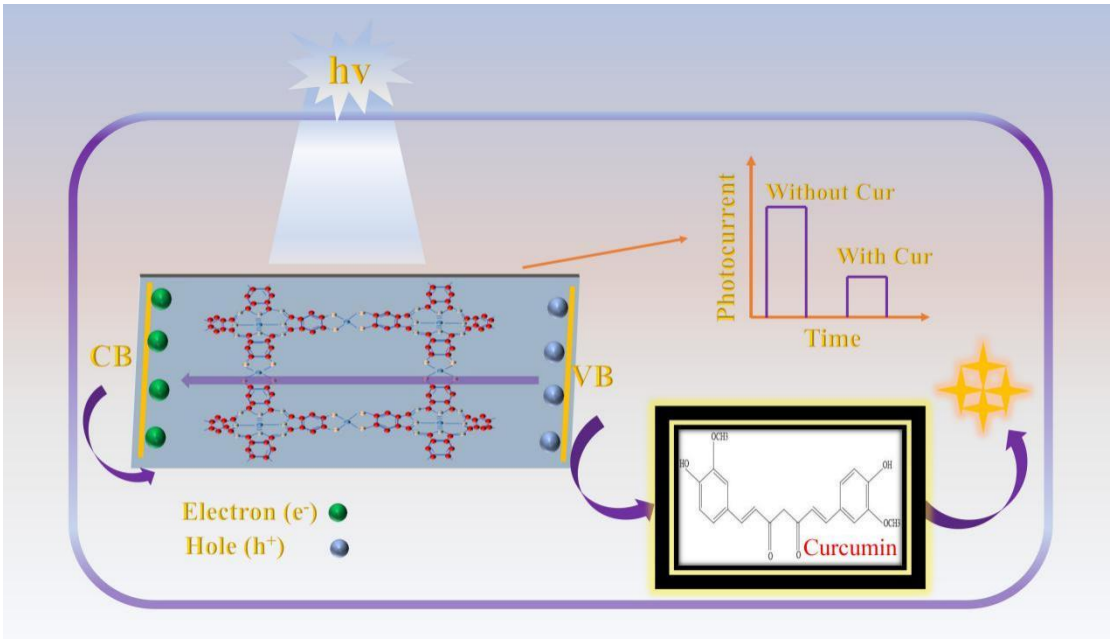

Scheme 2. Photoelectrochemical detection schematic diagram

3. RESULTS AND DISCUSSION

3.1 Characterization of NiPc–Ni MOF

The morphology of the synthesized NiPc–Ni MOF was characterized vis SEM and TEM (Fig. 1A and Fig. 1B, respectively). The synthesized NiPc–Ni MOF had an uneven surface composed of heterogeneous aggregates. TEM (Fig. 1B) showed that NiPc–Ni MOF had a nanoscale heterogeneous crystal structure.

Fig. 1C presents the FTIR spectra of the synthesized $(OH)_8$NiPc and NiPc–Ni MOF. Curve A revealed a strong absorption peak at 3416 cm^{-1}, which was assigned to the stretching vibration absorption peak of the O-H group. Thus, the methoxy group is reduced to the O-H group. The absorption peak at 1530 cm^{-1} was assigned to the C=C stretching vibration of the benzene ring skeleton.

The C-O stretching vibration was observed at 1278 cm^{-1}. In curve B, the hydroxyl stretching vibration was noted at 3400 cm^{-1}, which may be attribute to the presence of moisture in MOF material[37]. In addition, the stretching vibration for C=O and C-C can be seen.

Fig. 1D presents the XRD pattern of NiPc–Ni MOF. The XRD peaks of NiPc–Ni MOF were observed at 2θ =5.8°, 12.9°, and 26.2°, which were assigned to the (100), (200), and (001) planes of NiPc–Ni MOF, respectively. The peak positions concurred with those reported in the literature[38]. These characterization methods indicated that the NiPc–Ni MOF composite have been synthesized successfully .

The thermal stability of the NiPc–Ni MOF composite was tested by thermal gravimetric analyses (TGA). Fig 1E shows the TGA results of NiPc–Ni MOF. The NiPc–Ni MOF had excelled thermal stability at the temperature ranging from 0 to 345℃, and its mass loss was approximately 15%. The NiPc–Ni MOF mass loss accelerated with increasing temperature in the range of 345–485℃. NiPc–Ni MOF ceases to decompose when the temperature reaches 670℃. During the entire reaction, the total mass loss was approximate 68%.

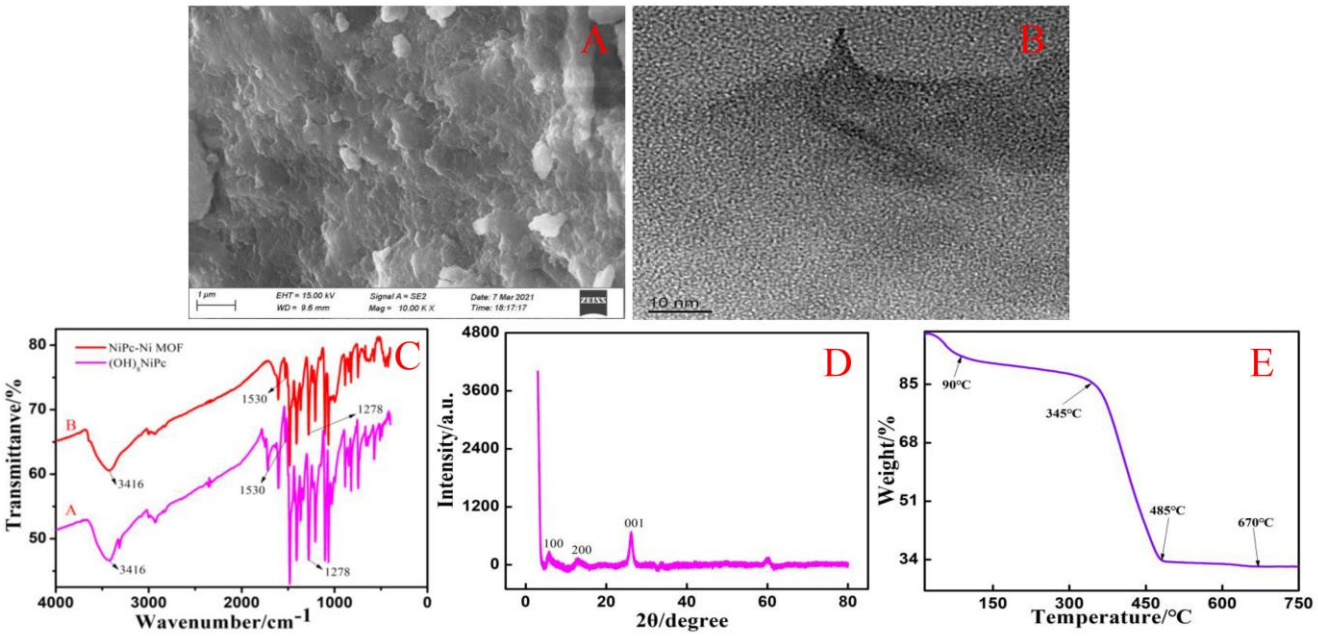

Figure 1. (A) SEM image of NiPc–Ni MOF . (B) TEM image of NiPc–Ni MOF. (C) FTIR spectra of $(OH)_8$NiPc and NiPc–Ni MOF. (D) XRD pattern of NiPc–Ni MOF. (E) TGA pattern of NiPc–Ni MOF.

3.2 Characterization of NiPc–Ni MOF

The electron transfer processes on bare/ITO, $(OH)_8$NiPc/ITO, and NiPc–Ni MOF/ITO, were examined by electrochemical impedance spectroscopy (EIS) in a 5-mM $K_3[Fe(CN)_6]/K_4[Fe(CN)_6]$ solution containing 0.1-M KCl. The frequency range was 1–100,000 Hz, and the amplitude was 0.005 V. The standing time was 2 s, and the initial potential was 0.329 V. The results are presented in Fig. 2A.

The Nyquist cure is usually made up of a straight line in the low-frequency region and a semicircle in the high-frequency region. The semicircle with larger diameter indicates greater impedance and slower electron transfer rate than others. As shown in Fig. 2A, bare/ITO had the largest semicircle diameter, followed by $(OH)_8$NiPc/ITO, and NiPc–Ni MOF/ITO. This means that NiPc–Ni MOF/ITO is suitable for electron transfer. The experimental results showed that NiPc–Ni MOF had been modified successfully on the ITO electrode.

The PEC signal intensities of the bare/ITO, $(OH)_8$NiPc/ITO, and NiPc–Ni MOF/ITO electrodes were studied in phosphate buffer solutions (PBS) containing 1.00×10^{-4} M Curcumin. The results are presented in Fig. 2B. The photocurrent of NiPc–Ni MOF was the largest in the absence of Curcumin, and the photocurrent was 4.560×10^{-7} A. Thus, NiPc–Ni MOF/ITO has an appropriate PEC response. After adding Curcumin to the electrolyte, the photocurrent of NiPc–Ni MOF/ITO decreased significantly. The decrease in the photocurrent indicates that the addition of Curcumin obstructs the electron transfer on the electrode surface.

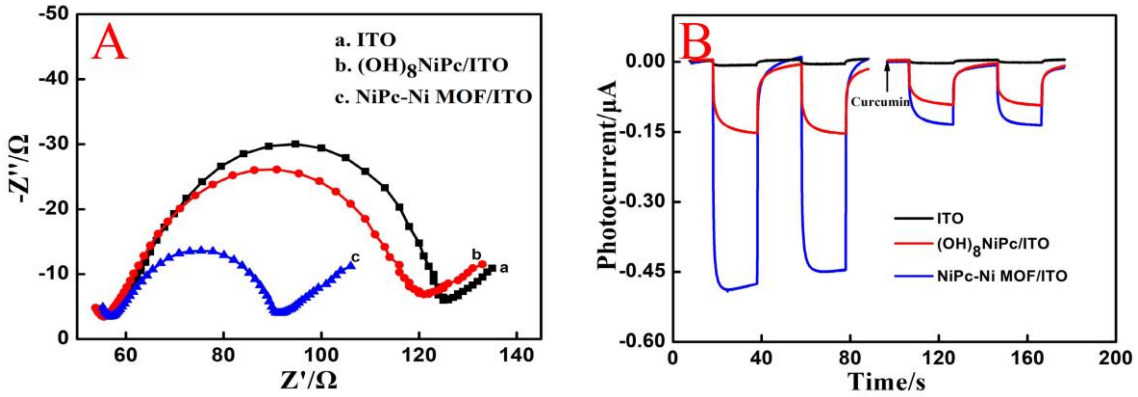

Figure 2. (A) EIS spectra of bare/ITO, $(OH)_8$NiPc/ITO, and NiPc–Ni MOF/ITO electrodes in a 5-mM $K_3[Fe(CN)_6]/K_4[Fe(CN)_6]$ solution containing 0.1-M KCl at frequency range of 1 – 100,000 Hz, amplitude of 0.005 V, standing time of 2 s, and initial potential of 0.329 V. (B) Photocurrent responses of bare/ITO, $(OH)_8$NiPc/ITO, and NiPc–Ni MOF/ITO electrodes in a 0.2 M PBS buffer solution (pH 7.0) at a potential of -0.1 V.

3.3 Optimization of experimental conditions

The light source, buffer solution, buffer solution pH, potential, modifier concentration, and coating amount were examined to optimize the experimental conditions. The influence of different light source, including yellow (λ: 570-600 nm), purple (λ: 365 nm), blue (λ: 420-470 nm), white (λ: 400-700 nm), red (λ: 620-630 nm), orange (λ: 420-470 nm), green (λ: 520-535 nm) light source (λ represents the spectral range, and the output power of light source is 20 mW/cm^2) on PEC response signal was examined in 0.2 M PBS buffer solution at a potential of -0.1 V. The results are shown in Fig. 3A. Under the irradiation of white light, the PEC sensor has the greatest response to Curcumin. Therefore, white light was used as the optimal light source in subsequent experiments. Fig. 3B shows the effect of different buffer solutions on the photocurrent response signal. Among the four buffer solutions, i.e., of 0.2 M PBS, HAc-NaAc, MBS, and B-R, the photocurrent was the highest in the PBS

buffer solution. Therefore, the PBS buffer solution was the optimal buffer solution. The effects of pH of the buffer solution on photocurrent in the range of 5.0~10.0 was studied in 0.2 M PBS buffer solution (Fig. 3C). In the range of pH 5.0~8.0, the photocurrent exhibited an upward trend and the maximum photocurrent was observed at pH 8.0. Thus, the optimal pH for the buffer solution was 8.0. Fig. 3D shows the effect of bias voltage on photocurrent response in the range of -0.4~0.2 V. As shown in Fig. 3D, the photocurrent increases and then decreases with the change of voltage. The photocurrent reaches the maximum value at -0.1 V. Hence, -0.1V was selected as the optimal voltage. The concentration of the modifier was optimized in previous optimal conditions (Fig. 3E). The photocurrent reached the maximum value when the modifier concentration was 2.5 mg mL^{-1}. Therefore, ITO electrodes modified with 2.5 mg mL^{-1} NiPc–Ni MOF materials were used in the experiments. Fig. 3F shows the effects of the coating amount on the electrode. The photocurrent was maximum when the amount of NiPc–Ni MOF was 25 μL. Therefore, the optimal amount of coating was 25 μL.

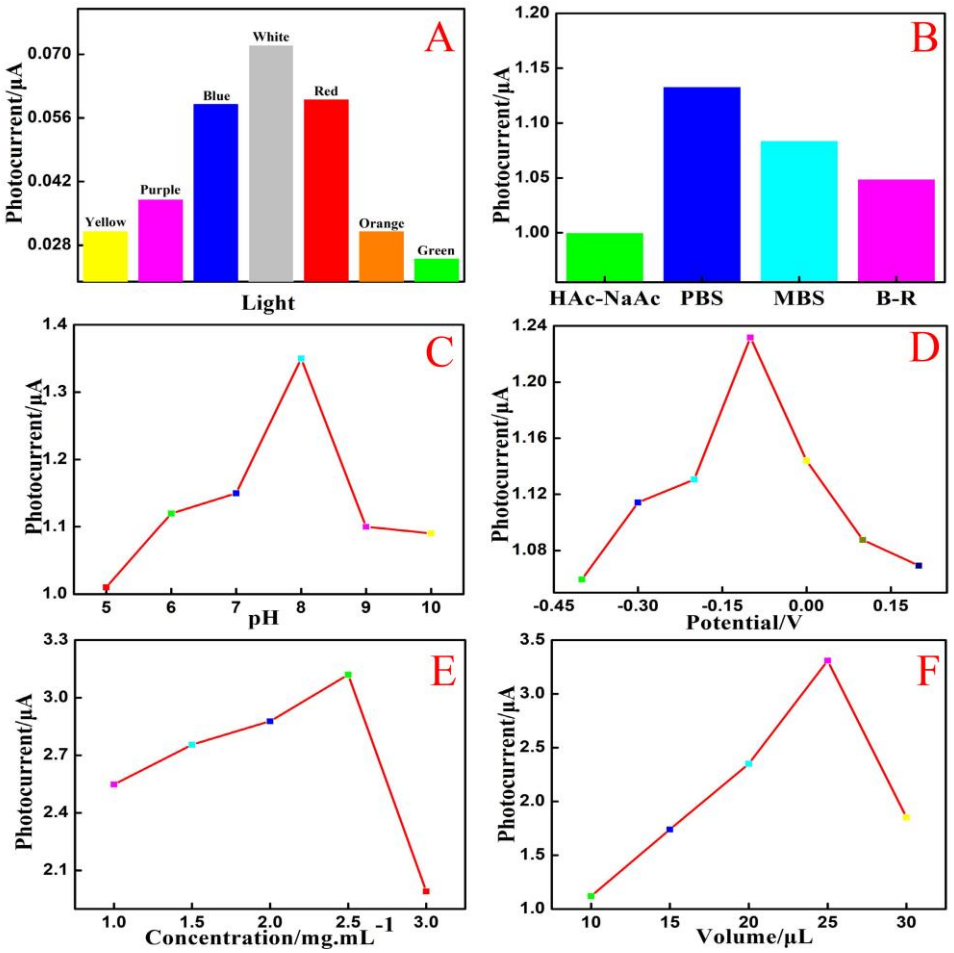

Figure 3. Effect of (A) different light source in 0.2 M PBS, (B) different buffer solutions, (C) electrolyte pH, (D) bias voltage, (E) concentration and (F) coating amounts of NiPc–Ni MOFon NiPc–Ni MOF/ITO response with 2.50×10^{-7} mol/L Curcumin.

3.4 PEC detection of Curcumin

Under the optimal experimental conditions, the PEC sensor was used to analyze Curcumin quantatively. Fig. 4A shows the PEC responses of NiPc–Ni MOF/ITO at Curcumin concentrations in the range of 0.0025–16 μM. The detection photocurrent decreased with increasing Curcumin concentration. This implied that the Curcumin molecules were associated with PEC process. Moreover, the photocurrent intensity decreased linearly with the increasing logarithm of Curcumin concentration ranging from 0.0025 to 16 μM. The linear regression equation was I= -0.0116lgC+0.0591 (R^2=0.9931). The estimated limit of detection (LOD=3S/k) was 0.8 nM. A comparing for Curcumin detecting of NiPc – Ni MOF/ITO with other electrodes was listed in Table 1. Compared with $LiClO_4$ [16], Carbon-SPE [17], Gr [18], MWCNTs [19] and TGA-CdTe@NiTAPcGr [3] modified electrode, the NiPc – Ni MOF/ITO showed wider linear ranger and lower detection limit. These results demonstrated that NiPc–Ni MOF/ITO is an integration platform appropriately for the determination of Curcumin.

Table 1. Determination of Curcumin by different methods.

Methods	Materials	Linear range (μM)	LOD (μM)	Ref.
EC	$LiClO_4$	9.9-107	4.10	[16]
EC	Carbon-SPE	2.2-280	4.90	[17]
EC	Gr	0.2-2.0-60	0.10	[18]
EC	MWCNTs	0.01-1.0	0.005	[19]
PEC	TGA-CdTe@NiTAPcGr	0.25-12.5-100	0.0125	[3]
PEC	NiPc–Ni MOF	0.0025-16	0.0008	This work

3.5 Reproducibility and stability of the PEC sensor

The reproducibility and stability of the sensor were studied under optimal experimental conditions. Five NiPc–Ni MOF electrodes were prepared for experimental study to investigate the reproducibility of the sensor. The PEC sensor has a small photocurrent difference. The relative standard deviation (RSD) was -3.24%. Therefore, the reproducibility of the sensor is relatively trustworthy. The short-term stability of the PEC sensor was examined using the concurrent method. The photocurrent of the modified electrode did not change substantially when the lamp was switched on 11 times continuously within 550 s (Fig. 4B). Therefore, the PEC sensor has good short-time stability. In addition, the long-term stability of the sensor was investigated by modifying the electrode and then storing it at room temperature. The changes in the photocurrent were measured at daily

intervals. The photocurrent did not change significantly and the RSD was -2.01% after 11 days (Fig. 4C). Therefore, the photocurrent has good long-term stability.

3.6 Selectivity of the PEC sensor for detection of Curcumin

The effects of possible interfering substances on the sensor were investigated to evaluate the selectivity of the PEC sensor. Potential interfering substances, such as amino acid, glucose, maltose, metal cation, and anion were studied. In the electrolyte containing Curcumin, interference substances were added and the changes before and after photocurrent were compared. These potential interfering substances did no interfere with the detection of Curcumin (Table 2). Therefore, the PEC sensor has excellent selectivity for detecting Curcumin.

Table 2. Effect of interfering substance on the detection of Curcumin

Interference	n	Er %	Interference	n	Er %
DL-alanine	100	-3.92	Dopamine	500	-4.83
L-valine	20	-1.36	Co^{+}	50	-3.09
L-threonine	100	-4.65	CO_3^{2-}	500	-3.48
L-phenylalanine	150	-4.48	NH_4^{+}	500	-3.48
L-arginine	100	-4.32	Fe^{3+}	350	4.90
L-glutamic acid	200	3.61	SO_4^{2-}	350	4.90
L-ascorbic acid	100	-3.82	Ca^{2+}	500	-3.85
L-cysteine	20	-4.33	Cl^{-}	500	-3.85
Maltobiose	200	-3.96	Ba^{2+}	500	-3.34
Glucose	20	-4.91	NO_3^{-}	500	-3.34
Sucrose	500	4.43	Mn^{2+}	20	4.42
Urea	50	-4.51	Pb^{2+}	20	-4.38
Oxalic acid	500	4.51	Na^{+}	100	-4.39
Glutathione	50	-2.79	K^{+}	250	-4.43
Lithic acid	50	-3.72	Br^{-}	250	-4.43
Ferulic acid	500	4.51	Li^{+}	500	3.10

3.7 Analysis of real samples

Swisse Curcumin tablets were used under optimal conditions to assess the utility of the sensor. The results were presented in Table 3. Parallel experiments were performed with a PEC sensor, and the RSD was 2.91%. The PEC sensor could detect Curcumin content in drugs. The accuracy of the PEC sensor was examined by HPLC (Fig. 4D), which confirmed it to be a feasible method for detecting Curcumin.

Table 3. Results of the determination of Swisse Curcumin in a real sample (n=3)

Real sample	HPLC (μM)	This method (μM)	RSD (%)
Swisse Curcumin	0.786	0.807	2.91

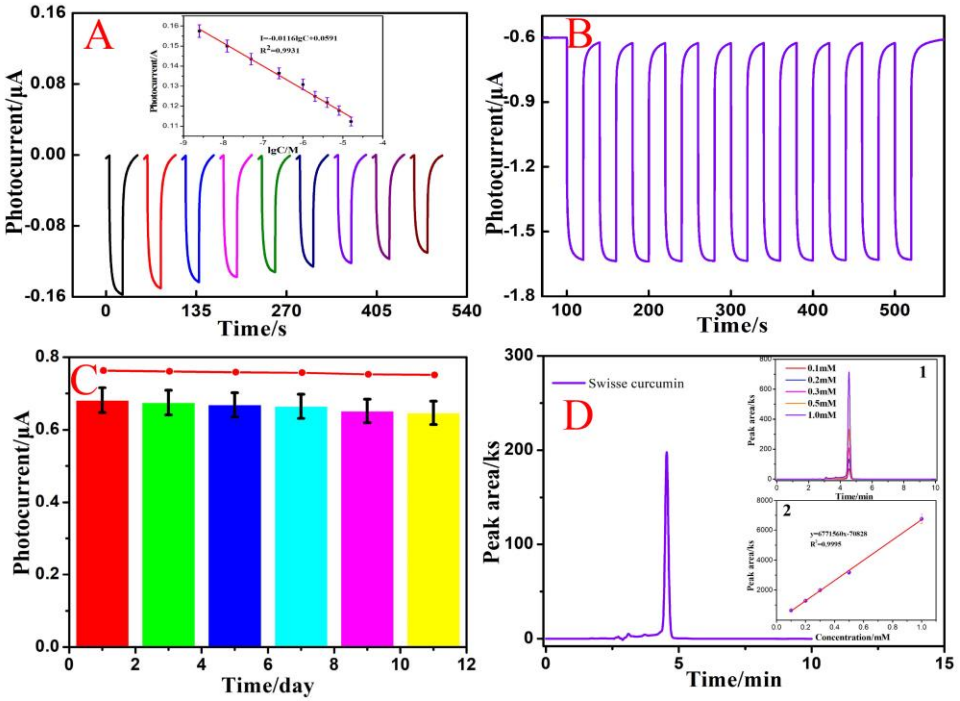

Figure 4. (A) PEC detection of Curcumin with NiPc–Ni MOF/ITO electrode in PBS 8.0. (B) Short-term stability of NiPc–Ni MOF/ITO electrode in PBS 8.0 with Curcumin under the lamp switched on 11 times within 550 s. (C) The photocurrent stability of Curcumin measured by NiPc–Ni MOF/ITO electrode within 11 days. (D) HPLC analysis results for Curcumin detection, illustrations 1 and 2 present the retention time-peak area pattern in the concentration range of 0.1-1.0 mM Curcumin and the standard curve, respectively.

4. CONCLUSIONS

A novel PEC sensor was developed to detect Curcumin by modifying an NiPc–Ni MOF on ITO electrodes. The sensor exhibited superior sensitivity and stability for detecting Curcumin. The linear response range of the sensor for detecting Curcumin was 0.0025–16 μM, and the detection limit was 0.8 nM. The sensor was applied to detection for Swisse Curcumin, and the results were accurate and reliable. Therefore, using this PEC sensor can be a new analytical method for the detection of Curcumin.

ACKNOWLEDGEMENT
This work supported by the Science Foundation Project of Liuzhou Institute of Technology (Grant No: 2021KXJJ01) and the Scientific Research and Innovation team Project of Liuzhou Institute of Technology (2018LSTD02).

References

1. J. Feng, Y. Li, Z. Gao, H. Lv, X. Zhang, D. Fan, Q. Wei, *Biosens. Bioelectron*., 99 (2018) 14.
2. F. Khan, N. Akhtar, N. Jalal, I. Hussain, R. Szmigielski, M. Q. Hayat, H. B. Ahmad, W. A. El-Said, M. Yang, H. A. Janjua, *Microchim. Acta*,186 (2019) 127.
3. J. Peng, Q. Huang, Y. Liu, P. Liu, C. Zhang, *Sens. Actuators, B*, 294 (2019) 157.
4. J. Peng, Q. Huang, W. Zhuge, Y. Liu, C. Zhang, W. Yang, G. Xiang, *Biosens. Bioelectron*., 106 (2018) 212.
5. J. Peng, W. Zhuge, Y. Liu, C. Zhang, W. Yang, Y. Huang. *J. Electrochem. Soc*., 166 (2019) B1612.
6. Y. Dou, J. Zhou, A. Zhou, J. -R. Li, Z. Nie, *J. Mater. Chem. A*, 5 (2017) 19491.
7. L. Huang, L. Zhang, L. Yang, R. Yuan, Y. Yuan, *Biosens. Bioelectron.*, 104 (2018) 21.
8. P. Anand, S. G. Thomas, A. B. Kunnumakkara, C. Sundaram, K. B. Harikumar, B. Sung, S. T. Tharakan, K. Misra, I. K. Priyadarsini, K. N. Rajasekharan, B. B Aggarwal, *Biochem. Pharmacol*, 76 (2008) 1590.
9. L. I. Nagy, L. Z. Fehér, G. J. Szebeni, M. Gyuris, P. Sipos, R. Alföldi, B. Ózsvári, L. H. Jr, A. Balázs, P. Batár, I. Kanizsai, L. G. Puskás, *BioMed Res. Int*., 2015 (2015) 11.
10. A. Kumar, S. Dhamgaye, I. K. Maurya, A. Singh, M. Sharma, R. Prasad, *Antimicrob. Agents Chemother.*, 58 (2014) 167.
11. L. Wing-Hin, L. Ching-Yee, B. Mary, L. Frederick, S. M. Rebecca, R. Ramin, Curr. Neuropharmacol., 11 (2013) 338.
12. R. S. P. Singh, U. Das, J. R. Dimmock, J. Alcorn, *J. Chromatogr. B*, 878 (2010) 2796.
13. R. A. Silva-Buzanello, A. C. Feroo, E. Bona, L. Cardozo-Filho, P. H. H. Araújo, F. V. Leimann, O. H. Gonçalves, *Food Chem.*, 172 (2015) 99.
14. W. Bian, X. Wang, Y. Wang, H. Yang, J. Huang, Z. Cai, M. M. F. Choi, *Luminescence*, 33 (2018) 174.
15. Z. Chen, L. Zhu, T. Song, J. Chen, Z. Guo, *Spectrochim. Acta, Part A*, 72 (2009) 518.
16. G. K. Ziyutadinova, A. M. Nizamova, H. C. Budnikov, *J. Anal. Chem.*, 67 (2012) 591.
17. D. M. Wray, C. Bathchelor-McAuley, R. G. Compton, *Electroanal.*, 24 (2012) 2244.
18. D. Zhang, X. Ouyang, J. Ma, L. Li, Y. Zhang, *Electroanal.*, 28 (2016) 749.
19. P. Daneshgar, P. Norouzi, A. A. Moosavi-Movahedi, M. R. Ganjali, E. Haghshenas, F. Dousty, M. Farhadi, *Electrochem.*, 39 (2009) 1983.
20. X. Zhang, R. Tu, Z. Lu, J. Peng, C. Hou, Z. Wang. Coord. Chem. Rev., 443 (2021) 214032.
21. V. Agostoni, P. Horcajada, M. Noiray, M. Malanga, A. Aykaç, L. Jicsinszky, A. Vargas- Berenguel, N. Semiramoth, S. Daoud-Mahammed, V. Nicolas, C. Martineau, F. Taulelle, J. Vigneron, A. Etcheberry, C. Serre, R. Gref, *Sci. Rep.*, 5 (2015) 7925.
22. Y. Tang, S. Tanase, *Microporous Mesoporous Mater.*, 295 (2020) 109946.
23. T. Li, Y. Bai, Y. Wang, H. Xu, H. Jin, *Coord. Chem. Rev.*, 410 (2020) 213221.
24. S. Carrasco, *Biosens.*, 8 (2018) 92.
25. J. Peng, C. Hou, X. Hua. *Sens. Actuators, B*, 169 (2012) 81.
26. J. Y. Peng, C. T. Hou, X. X. Liu, H. B. Li, X. Y. Hu. *Talanta*, 86 (2011) 227.
27. F. Liu, Q. Xu, W. Huang, Z. Zhang, G. Xiang, C. Zhang, C. Liang, H. Lian, J. Peng. *Electrochim. Acta*, 295 (2019) 615.
28. T. T. Tung, M. T. Tran, J. Feller, M. Castro, T. V.n Ngo, K. Hassan, M. J. Nine, D. Losic. *Carbon*, 159 (2020) 333.

29. A. Bag, M. Kumar, D. Moon, A. Hanif, M J. Sultan, D. H. Yoon, N. Lee. *Sens. Actuators, B*, 346 (2021) 130463.
30. M. Yu, J. Liu, C. Liu, W. Pei, J. Ma. *Sens. Actuators, B*, 347 (2021) 30604.
31. Z. Xia, B. Shi, W. Zhu, C. Lü. *Chem. Eng. J*., 426 (2021) 131794.
32. L. Wang, P. Jin, S. Duan, H. She, J. Huang, Q. Wang. *Sci. Bull*., 64 (2019) 926.
33. J. Kim, S. Yeo, J. D. Jeon, S. Y. Kwak, *Microporous Mesoporous Mater.*, 202 (2015) 8.
34. H. Nagatomi, N. Yanai, T. Yamada, K. Shiraishi, N. Kimizuka, *Chem. Eur. J*., 24 (2018) 1806.
35. H. Jia, Y. Yao, J. Zhao, Y. Gao, Z. Luo, P. Du, *J. Mater. Chem. A*, 6 (2018) 1188.
36. L. Xu, S. Ling, H. Li, P. Yan, J. Xia, J. Qiu, K. Wang, H. Li, S. Yuan, *Sens. Actuators, B*, 240 (2017) 308.
37. F. N. Azad, M. Ghaedi, K. Dashtian, S. Hajati, V. Pezeshkpour, *Ultrason. Sonochem.*, 31 (2016) 383.
38. Z. Meng, A. Aykanat, K. A. Mirica, *J. Am. Chem. Soc.*, 141 (2019)2046.

© 2022 The Authors. Published by ESG (www.electrochemsci.org). This article is an open access article distributed under the terms and conditions of the Creative Commons Attribution license (http://creativecommons.org/licenses/by/4.0/).